مجلة المنتدى الأكاديمي (العلوم التطبيقية)
المجلد (7) العدد (2) يوليو 2023
ISSN (Print): 2710-446x , ISSN (Online): 2710-4478
تاريخ التقديم: 2023/06/16 ، تاريخ القبول: 2023/07/20، تاريخ النشر: 2023/07/25

EXPRESSION of MOLT-INHIBITING HORMONE in BRAIN and THORACIC GANGLION of *Carcinus maenas*

Ali Moftah Abuhagr

Department of Histology & Genetics, Faculty Medicine, Alasmarya Islamic University, Libya.

E-mail: aliabuhagr@asmarya.edu.ly

Abstract

Decapod crustacean eyestalks produced the neuropeptide hormone known as "molt inhibiting hormone (MIH) which controls molting by blocking the Y-organ's to make ecdysteriods (molting hormones). Typically, eyestalk ablation (ESA) can trigger molting. However, adult green crabs (*Carcinus maenas*) are resistant to ESA. ESA generates a slight rise in hemolymph ecdysteroid titers, although animals do not instantly enter premolt. Some ES-ablated animals molt after several months, while the majority do not molt at all. We suspected that MIH came from other parts of the nervous system, notably the brain and/or the thoracic ganglion. MIH transcript is present in the brain and thoracic ganglions of intermolt crabs using nested endpoint RT-PCR. The PCR products identify as MIH was verified by sequencing. The effects of ESA on MIH expression were investigated using quantitative PCR. The thoracic ganglion and brain of both the green and red color morphs were harvested at 7 days and 14 days post-ESA. Animals' intact tissues were used as controls. MIH expression was similar between the color morphs and ESA had little effect on MIH transcript levels, indicating that the loss of the eyestalks did not affect the transcriptional regulation of the MIH gene. The data indicate that when the main supply of MIH is eliminated by ESA, MIH released by brain and/or thoracic ganglion neurons is sufficient to prevent molt induction.

Key words*:* MIH- Crustaceans- Ecdysteroid- Thoracic ganglion- Eyestalk ablation, ESA.

Introduction :

The green crab, *Carcinus maenas*, has spread to protected coastal and estuary environments all around the world (Grosholz and Ruiz, 1996; Hanfling et al., 2011). According to genetic analysis, the two color morphs of adults that are present differentiate by the pigmentation on the ventral side of the thoracic segments and the arthrodial membrane connecting the basal segments of each leg (Tepolt et al., 2009). When an animal ages, red pigmentation in the leg joints extends over the ventral surface in "red" morphs, while "green" morphs have a pale green ventral surface and leg joints (McGaw and Naylor, 1992a). Green morphs molt more regularly from February to April and are more prevalent in the winter. The red morphs, which are more prevalent in the fall, develop from the green morphs over the summer. Ecophysiological characteristics vary amongst color variants in populations. Red morphs mostly live in the subtidal zone, and they can't endure low salinity for long (McGaw et al., 1992; McGaw and Naylor, 1992a, b). Green morphs are more common in salt marshes and the high intertidal zone and can survive a wider variety of salinities (McGaw et al., 1992; McGaw and Naylor, 1992a, b). Red morphs molt less frequently and devote more energy to reproduction, whereas green morphs spend more energy growing and molting. Red morphs have thicker exoskeletons and stronger claws as a result of the longer intermolt interval (Reid et al., 1997; Taylor et al., 2009).

When crustaceans ecdysis, or molt, physiological processes in various organs and tissues must be precisely coordinated. For example, the breakdown of the old exoskeleton, the synthesis of a new exoskeleton, the regeneration of lost appendages, and the atrophy of skeletal muscle in the claws are just a few examples (Chang and Mykles, 2011; Mykles, 1997; Skinner, 1985). The four main phases of the molt cycle are intermolt, premolt, ecdysis, and postmolt (Skinner, 1985). These activities are started and coordinated by steroid molting hormones called ecdysteroids, which are produced and released by a pair of molting glands called Y-organs (YOs) (Lachaise et al., 1993; Skinner, 1985). Thus, the YOs, located in the anterior cephalothorax, are triggered to initiate the shift from the intermolt stage to the premolt stage (Chang and Mykles, 2011). Ecdysteroid levels in the hemolymph are low throughout the post- and intermolt phases and rise during premolt, peaking towards the end of premolt (Chang, 1989; Mykles, 2011). A few days before to ecdysis, there is a significant decline in ecdysteroid levels, which acts as a catalyst for the exoskeleton's actual shedding (ecdysis), as well as for the development of the claw muscles and the synthesis and calcification of the exoskeleton during the postmolt stage (Chang and Mykles, 2011; Skinner, 1985).

The X-organ/sinus gland (XO/SG) complex, which is found in the eyestalks of decapod crustaceans, produces inhibitory neuropeptides that regulate the YOs (Chang and Mykles, 2011; Hopkins, 2012; Skinner, 1985; Webster et al., 2012). These neuropeptides, crustacean hyperglycemic hormone (CHH) and molt-inhibiting hormone (MIH), prevent the YO from producing ecdysteroid hormones (Chang and Mykles, 2011; Covi et al., 2012; Nakatsuji et al., 2009; Webster et al., 2012). However, there have been a few instances of MIH expression in tissues outside of the XO/SG complex (Lu et al., 2001; Tiu and Chan, 2007; Zhu et al., 2011). Comparatively, the XO/SG complex, among many

other tissues, expresses CHH (Webster et al., 2012). Inhibiting ecdysteroid production through cGMP-dependent signaling pathways, both neuropeptides have comparable, highly conserved motifs (Covi et al., 2009; Mykles et al., 2010). Eyestalk ablation (ESA) or multiple leg autotomy (MLA), which involves the removal of at least five walking legs, can cause molting in the majority of decapod crustaceans (Chang and Mykles, 2011; Mykles, 2001; Skinner, 1985). After ESA eliminates the main cause of MIH, the YO is immediately activated, and hemolymph ecdysteroid titers rise within a day (Covi et al., 2010; Lee et al., 2004; Lee et al., 2007b; Lee and Mykles, 2006).

The purpose of this study was to investigate the effects of ESA and MLA on molting and YO gene expression in the two color morphs across intermediate and long time periods. We predicted that red morphs would be less susceptible to molt induction than green morphs as red morphs molt less frequently. By using nested PCR and qPCR, the expression of MIH in the brain and thoracic ganglia in intact and ESA green and red morphs was identified. The findings demonstrated that both color morphs are resistant to ESA and MLA and that the brain and thoracic ganglia are secondary sources of MIH.

Materials and Methods:

Mature male green crabs (*Carcinus maenas*) were collected from Bodega Bay's port. They were kept in Bodega Marine Laboratory facilities under ambient settings of around 13°C and fed squid twice a week. They were given cooked chicken liver once a week, and their water was replaced after feeding. ESA and MLA used the same techniques for *G. lateralis* (Lee et al., 2007a; Skinner and Graham, 1972). YOs from animals (green morphs) undergoing normal molts were collected and extracted from intermolt, premolt, and postmolt animals, frozen in liquid nitrogen, and preserved at -80 ˚C. Hemolymph samples (100 µl) were collected at the moment of tissue harvest and mixed with 300 µl methanol for ELISA. Interval tests were used to investigate the effects of ESA in green and red morphs for up to 24 days. YOs were collected from intact (Day 0) animals as well as ESA animals at various post-ESA intervals. Hemolymph samples (100 µl) were collected at harvest and mixed with 300 µl methanol for ELISA.

Long-term experiments in green and red morphs determined the effects of ESA and MLA after around 3 months. Green morph animals were separated into three treatment groups during the winter molting season: intact control (n = 10), ESA (n = 9), and MLA (n = 18). In the MLA group, all eight walking legs were autotomized. Every two weeks, digital photographs of the ventral portion of each crab were taken. Pictures were processed with Photoshop CS software using the "Info" tab to measure the intensities of red, green, and blue from the crab's left side's middle of first thoracic sternum. Results were analyzed by one-way analysis of variance (ANOVA) using Sigmastat version 3.00 (SPSS, Inc.). In the late spring season, red morph animals were separated into four treatment groups: intact control (n = 3), ESA (n = 4), MLA (n = 4), and ESA Plus MLA (n = 4). Every week, 50 µl of hemolymph was mixed with 350 µl of methanol for ELISA. The YOs were collected after around 90 days kept at -80 ˚C.

Ecdysteroid ELISA:

The ELISA for ecdysteroid was modified from (Kingan, 1989) and Tamone et al., 2007). Plates (96-well, Costar 3366, Corning, NY, USA) were coated for 2 hours at 23 ˚C with AffiniPure goat anti-rabbit IgG Fc fragment antiserum (Jackson ImmunoResearch Labs 111-005-008, West Grove, PA, USA; 0.5 g in 90 l per well) in phosphate-buffered saline (PBS; 10 mM sodium phosphate, 0.15 mM NaCl. The wells were incubated (300 µl per well) with assay buffer (AB; 25 mM sodium phosphate, pH 7.5; 150 mM NaCl; and 1 mM EDTA disodium dihydrate) containing 0.1% bovine serum albumin (BSA, Fraction V; Sigma A-9647, St. Louis, MO, USA) for 2 h at 23 ˚C. The wells were washed 3 times with PBS containing 0.05% Tween 20 (PBS-T; Sigma, P-5927). All samples were run in duplicate. Nonspecific binding (NSB) was determined by loading wells with AB containing 0.1% BSA (100 µl per well). Standards ranged from 0 to 120 pg 20-hydroxyecdysone (20E) in AB containing 0.1% BSA (50 µl per well). Hemolymph samples in methanol were centrifuged for 10 min at 20,000 xg at 4 ˚C to remove precipitated protein. Supernatant aliquots (10 µl) were dried under vacuum in a Speed Vac centrifuge (Savant, West Palm Beach, FL, USA) and dissolved in 150 µl AB containing 0.1% BSA. Samples (50 µl), in duplicate, were loaded into each well. An internal standard consisting of lobster (*Homarus americanus*) hemolymph was included to assess inter-assay variation. 20E conjugated to horseradish peroxidase (HRP) reagent (1:64,000 dilutions in AB with 0.1% BSA; 50 µl) was added to all wells and incubated for 5 min at 23 ˚C. A rabbit anti-ecdysteroid primary antibody (50 µl; 1: 100,000 dilutions in AB with 0.1% BSA) was added to all wells, except for the first two wells containing NSB. The 20E/HRP conjugate and 20E antibody were obtained from Dr. Timothy Kingan. The plates were sealed with Parafilm and incubated overnight at 4 ˚C.

Equal volumes of Solutions A and B of a tetramethylbenzidine-peroxidase (TMB) kit (KPL, catalog 50-76-03, Gaithersburg, MD, USA) were combined and 100 µl were added to each well. The plates were incubated for 15 min at 23 ˚C in the dark. The reaction was stopped by the addition of 100 µl 1 M phosphoric acid and read with a Genios plate reader (Tecan, San Jose, CA, USA) at 450 nm. The data were archived with Magellan 6 and analyzed with Microplate Manager (Bio-Rad) software.

RT-PCR and RNA isolation:

The RNA isolation procedure is explained in (Covi et al., 2010). Prior to dissecting the YO and other tissues, animals were given a 5-minute ice anesthesia. For ecdysteroids to be quantified by radioimmunoassay (Medler et al., 2005) or ELISA, hemolymph samples (100 µl) were mixed with 300 µl methanol. Liquid nitrogen was used to freeze the tissues, which were then kept at -80 °C. Utilizing the manufacturer's instructions, total RNA was isolated using the TRIzol reagent (Invitrogen, Carlsbad, CA, USA). Total RNA was processed with DNAase I for 30 min, extracted using phenol:chloroform:isoamyl alcohol (25:24:1), precipitated with 1 volume of isopropanol, and dissolved in 30 µl nuclease-free water. Using a NanoDrop ND-1000 Spectrophotometer from Thermo Fisher Scientific, Inc., the amount of RNA was measured by absorbance at 260 nm. cDNA was synthesized in reactions (20 µl) containing 1 µg RNA, 4 µl of Roche's Transcriptor RT reaction buffer, 0.5 µl of Fermentas' Ribolock RNase Inhibitor (40 u/l), 0.5 µl of Roche's

reverse transcriptase, 2.0 µl of dNTP (10 mM), and 5 µl of nuclease-free water. RNase H was used to remove complementary RNA. End-point PCR was used to assess the tissue distribution of *C. maenas Cm-MIH* GenBank accession # X75995; (Klein et al., 1993), and *Cm-Elongation Factor-2* (*Cm-EF-2*; #GU808334). The reactions' master mix 2 included 1µl of template cDNA and 5 pmol of each of the suitable expression primers (Table 1) 30 or 35 cycles of 94°C for 30s, the lowest annealing temperature of a primer pair for 30s, and 72°C for 30s were completed after 3 minutes of 94°C denaturation. The last extension lasted 7 minutes at 72°C. Products were separated on a 1% agarose gel containing TAE (40 mM Tris acetate and 2 mM EDTA, pH 8.5) after the PCR process was completed. The gels were stained with ethidium bromide and examined under a UV light source. The control for RNA isolation and cDNA synthesis was provided by the constitutively expressed "housekeeping" gene *Cm-EF-2*.

(Table 1): Primers used for *Cm-MIH* and *Cm-EF2* qPCR: Cm, *C. maenas*; F, forward; R, reverse.

Primer	Sequence (5' to 3')	Product Size	Annealing Temperature
Cm-EF2 F1	CCATCAAGAGCTCCGACAATGAGCG	278 bp	61˚C
Cm-EF2 R1	CATTTCGGCACGGTACTTCTGAGCG		61˚C
Cm-MIH F1	TATCGGTGGTGGTTCTGG	281 bp	54 ˚C
Cm-MIH R1	AGCCCCAAGAATGCCAACC		58˚C
Cm-MIH F2	CGGCGAGAGTTATCAACG	199 bp	53˚C
Cm-MIH R2	TCTCTCAGCTCTTCGGACC		53˚C

The quantitative analysis of *Cm-MIH*, and *Cm-EF-2* was carried out using a Light Cycler Fast Start DNA Master Plus SYBR GREEN I reaction mix and a Light Cycler 480 heat cycler from Roche Applied Science. qPCR reactions contained 1 µl cDNA, 5 µl 2x SYBR Green Master Mix, 0.5 µl (10 mM) each of forward and reverse gene-specific primers (Table 1), and 3 µl of PCR-grade water. For *Cm-MIH* and *Cm-EF-2*, standard curves were created by serially diluting purified PCR products (10^{-8} ng/µl to 10^{-16} ng/µl). The PCR experiments used Master Mix 2 from Thermo scientific and comprised 1 l of template cDNA and 5 pmol of each suitable expression primer (Table 1). In order to reduce the variance of the mean, all qPCR data were log transformed. An analysis of variance (ANOVA) was used to compare the means of transcript abundance for days post-ESA verses log copy number. The means of naturally molting animals in various molting phases were contrasted with log copy numbers using an ANOVA. The means for transcript abundance between red and green morph hemolymph ecdysteroid concentration verses log copy number were compared using a paired t-test. To identify outliers, a Grubb's test was applied. For all data analysis, the threshold of significance was fixed at $\alpha = 0.05$.

Results and Discussion :

Effects of ESA and MLA on hemolymph ecdysteroid in YOs from the red and green morphs:

The effects of ESA on hemolymph ecdysteroid levels was examined in green morphs over a 16-day period and red morphs over a 24-day period. ESA caused a brief increase in ecdysteroid titers, although the magnitude and timing of the color morphs varied (Fig. 1A). The ecdysteroid concentration in red morphs increased by 4.2 fold to 48.9 pg/ µl at 14 days after ESA ($P < 0.0001$), and then decreased by 3.8 fold ($P < 0.0001$) at 21 days after ESA (Fig. 1A). Hemolymph ecdysteroid in green morphs increased by a factor of two to 20.5 pg/ µl (P 0.012) at 3 days after ESA before reverting to pre-ESA values at 14 and 21 days after ESA. Hemolymph ecdysteroid levels in green morphs increased by twofold to 20.5 pg/ µl (P 0.012) at 3 days after ESA before dropping to pre-ESA values at 14 and 21 days after ESA (Fig. 1A). The constitutively expressed control gene *Cm-EF2* in the green and red morphs was not significantly impacted by ESA (Fig. 1B). Additionally, in neither color morph did hemolymph ecdysteroid concentration significantly correlate with *Cm-EF2* mRNA levels.

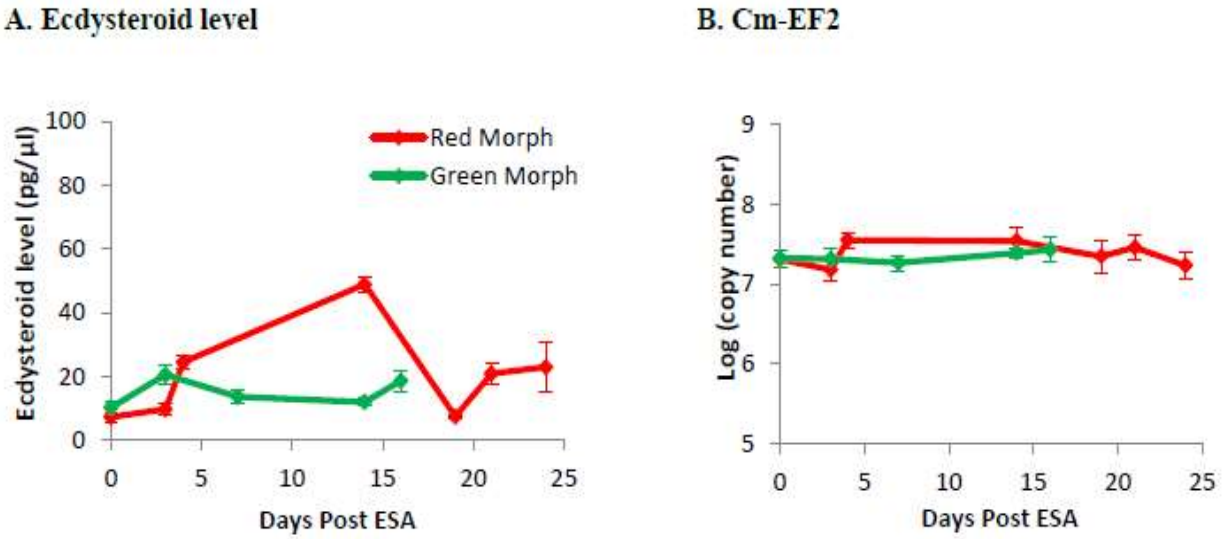

Figure (1): Effects of ESA on hemolymph ecdysteroid (**A**) and EF2 expression (**B**) in red (red symbol and line) and green (green symbol and line) morphs over 24 and 16 days, respectively. Animals were eyestalk-ablated at Day 0. YOs were harvested and hemolymph samples were taken at various intervals post-ESA. Ecdysteroid levels were quantified by ELISA. mRNA levels were quantified by real-time PCR. Data presented as mean ± 1. S.E. (red morph, n = 3 at Days 3 and n = 6 at Days 14; green morph, n = 4 at Days 7 and n = 6 at Days 3).

Long-term experiment: The long-term effects of ESA and MLA were determined on red and green morphs. Four treatment groups were created from the red morphs: intact (control), ESA, MLA, and combined ESA+MLA. In the summer, following the winter/spring molting season, the experiment was conducted. All of the red morphs were at the intermolt stage when the experiment began and stayed there for the entire 90-day period; no animals underwent molting. ESA substantially raised hemolymph ecdysteroid levels at Day 28 and subsequent time points, either alone or in combination with MLA, although the means never exceeded 30 pg/µl (Day 45; Fig. 2). There was no significant difference between the intact and MLA animals, except at Day 52 (Fig. 2).

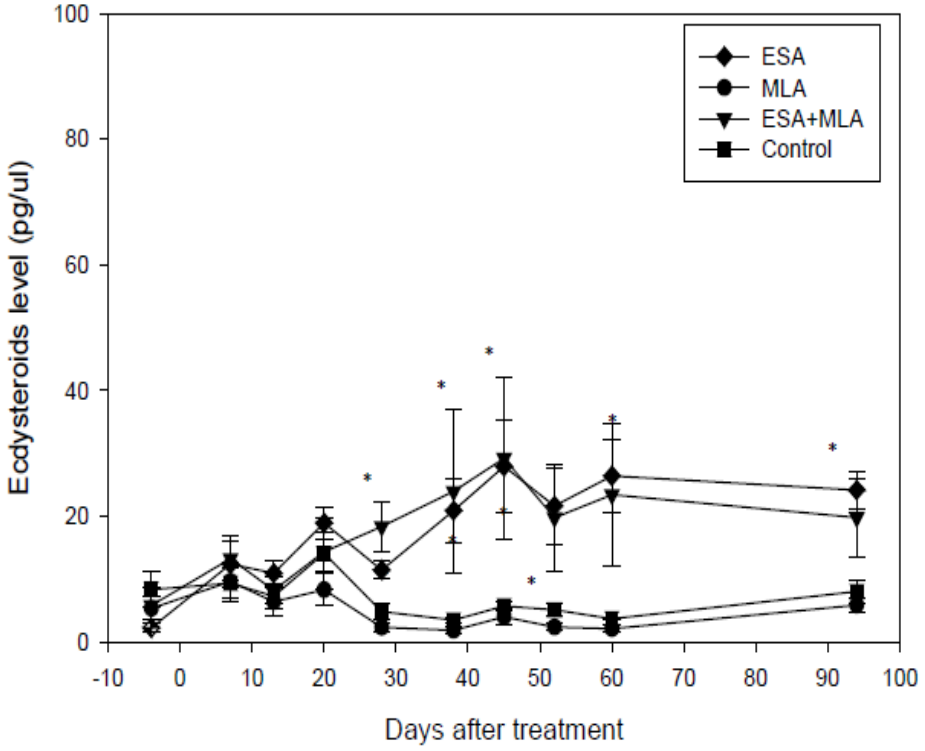

Figure (2): Effects of ESA and MLA on ***C. maenas*** hemolymph ecdysteroid levels in red morphs.

Intermolt red morphs were divided into intact (control), ESA, MLA, and ESA+MLA treatment groups and hemolymph samples were taken at weekly intervals during the 3-month period. Data presented as mean ± 1. S.E. (n=5).

Green morphs were split into three treatment groups : intact (control), ESA, and MLA. The experiment was started in February at the start of the molting season. Weekly hemolymph samples were collected, and ecdysteroid titers were measured at the end of the experiment. Eight of the 30 animals were in premolt at Day 0:2, as seen by higher ecdysteroid levels (between 72.0 and 196.0pg/µl) in the control, MLA, and ESA groups.

The premolt animals' molting was unaffected by MLA; ecdysteroid levels continued to rise in both the premolt intact and MLA animals, and all five animals molted within four weeks (Fig. 3; compare A and B). ESA, in contrast, delayed the molting of premolt animals. Two of the animals, who molted at Days 40 and 90, had delayed increases in hemolymph ecdysteroids; the third animal, however, saw decreased in ecdysteroid titer and did not molt during the experiment (Fig. 3C). For the duration of the experiment, the other 22 animals that were in intermolt on Day 0 did not molt. The hemolymph ecdysteroid levels were unaffected by MLA since there were no significant changes in the means of the intact and MLA animals at any time points, except at Day 63 (Fig. 3D). In

contrast, ESA significantly raised hemolymph ecdysteroid levels at Day 21 and following time points, while the means never exceeded 53 pg/µl (Day 70; Fig. 3D).

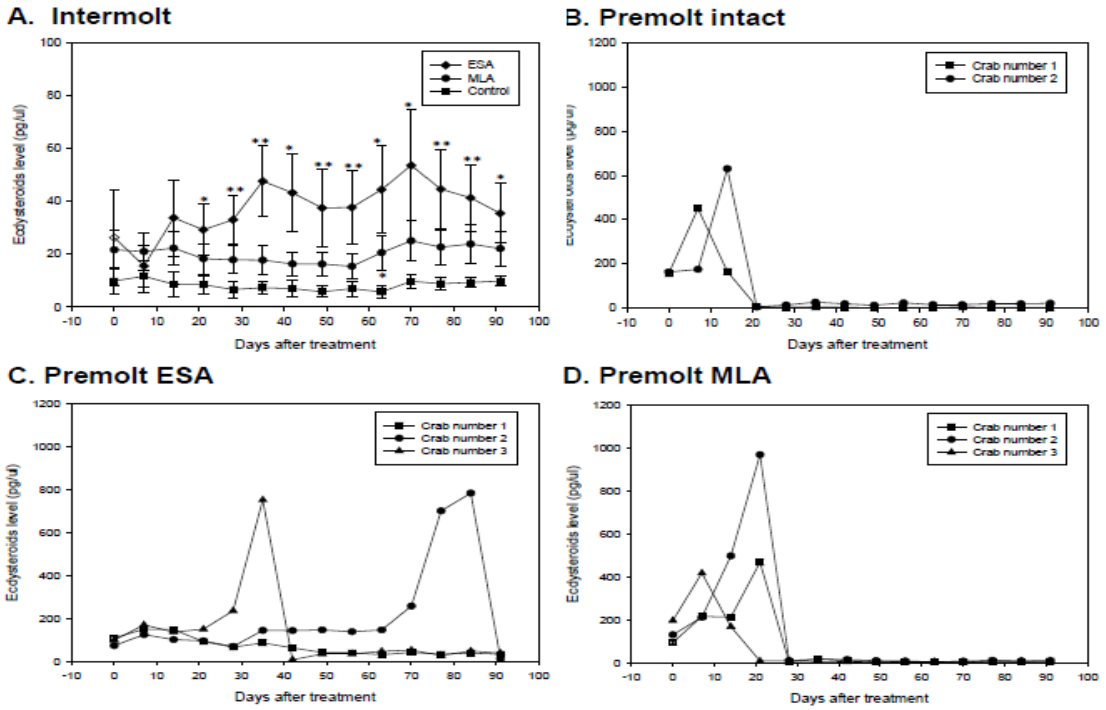

Figure (3): Effects of ESA and MLA on ***C. maenas*** hemolymph ecdysteroid levels in green morphs. Green morphs were divided into intact, ESA, and MLA treatment groups and hemolymph samples were taken at weekly intervals during the 3-month period. Intermolt animals at Day 0 are graphed in (A); data presented as mean ± 1. S.E. (intact, n = 10; ESA, n=7 and MLA n=18). Premolt animals at Day 0 are graphed separately for individual crabs: (B) intact animals; (C) ESA animals; and (D) MLA animals.

We observed that ESA accelerated the transition from the green to red color morph pigmentation when doing the intermediate-interval experiments on the green morphs. In the long-term experiment, this shift was captured using digital photographs of intact, MLA, and ESA animals' ventral cephalothoraxes at 2-week intervals (Fig. 4 A). By 4 weeks post-MLA, there was a noticeable reddening of the arthrodial membranes of the basi-ischial joints, compared to those of the intact animals. Six to twelve weeks after MLA, the ventral cephalothorax also showed a slight reddening. Within two weeks of starting ESA, red pigment began to build up in the ventral cephalothorax and basi-ischial joints, and the red color became more intense at later time intervals (Fig. 4 A). All of the animals' photos were examined to look for variations in the ventral exoskeleton's red, blue, and green hues. Since green color was impacted by treatment while red and blue colors remained largely constant, the results are shown as the ratio of green to red intensities. The ratio of green to red colors was considerably reduced by ESA (Fig. 4 B). Additionally, there was a decline in the green

to red ratio in MLA animals, but the means did not differ significantly from those of intact animals. In light of the red pigment found in the exoskeleton, we conclude that ESA caused a loss of green color. Following the long-term experiments, YOs were harvested, and real-time PCR was used to quantify the expression of EF2 (Fig. 4). For Cm-EF2 examined in red and green morph, ESA and MLA experiments revealed little change. EF2 copy numbers expressed in YOs tissue in the red or green morph did not significantly alter.

A.

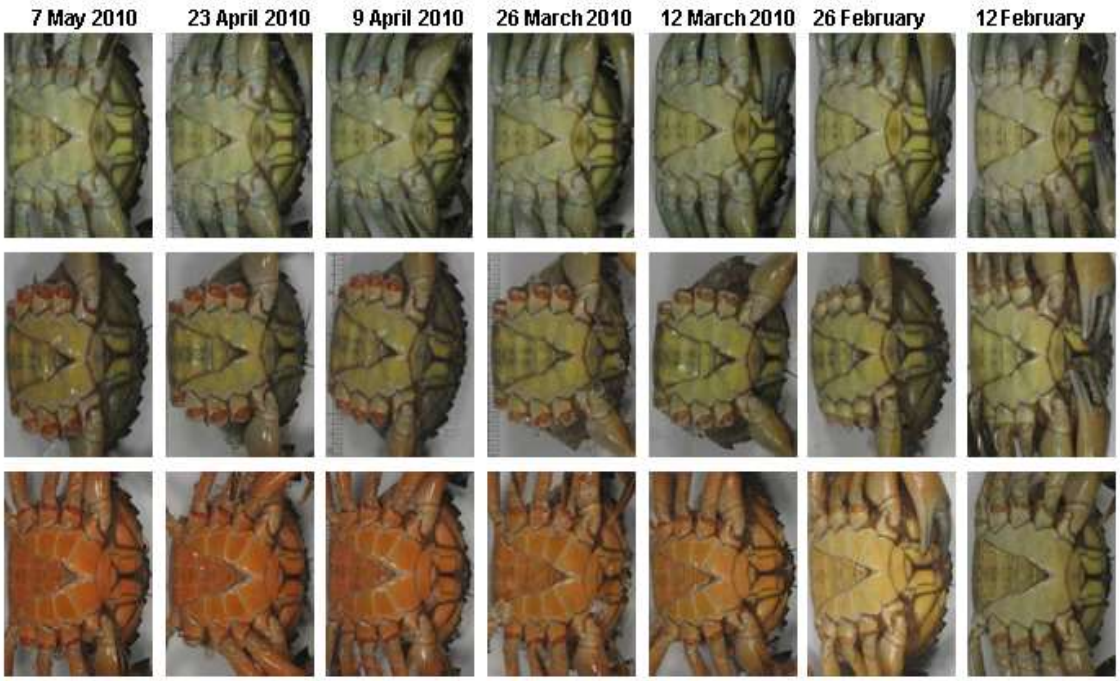

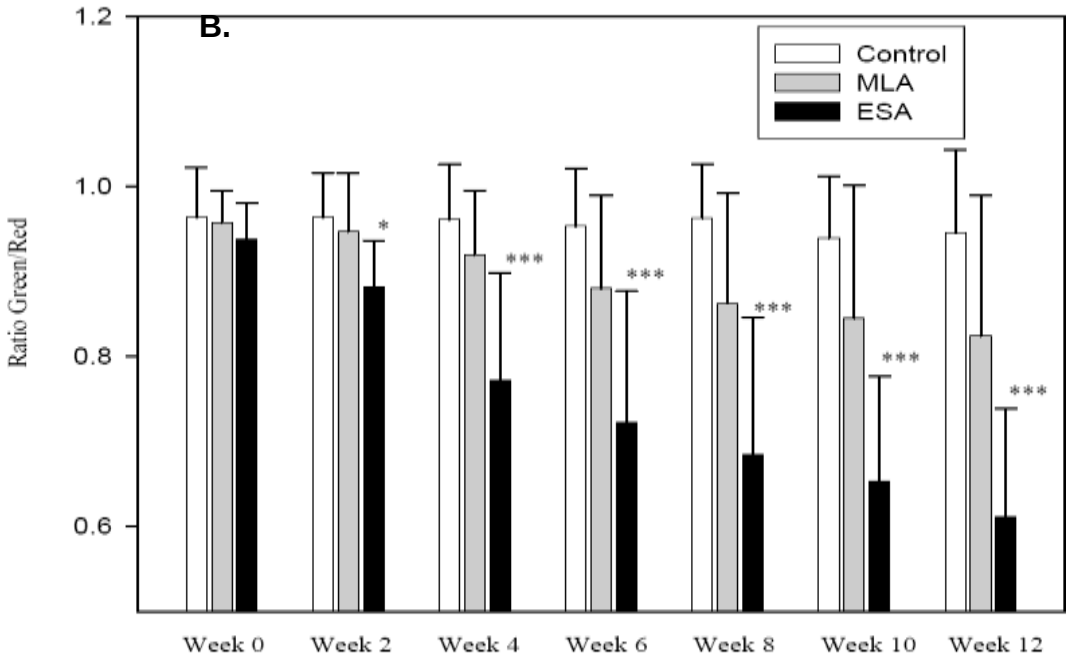

Figure (4): Effects of eyestalk ablation (ESA) and multiple leg autotomy (MLA) on *C. maenas* green morph ventral pigmentation. (A) Representative images of individual animal from intact, ESA, and MLA treatment groups captured at 2-week intervals for 12 weeks. Approximate width of each panel is equivalent to 5 cm. (B) Ratio of green to red color intensities of the left thoracic sternum of intact (n = 10), ESA (n = 10), and MLA (n = 20) animals (mean ± 1 S.D.; see Materials and methods). Asterisks indicate significant differences between the control and ESA crabs at $p < 0.05$ (*) and $p < 0.001$ (***). There were n o significant differences between the intact and MLA animals.

Effects of molting on YO expression of EF2 and hemolymph ecdysteroid in brain and thoracic ganglion from green and red morphs:

During the natural molt cycle stages (intermolt, premolt, and postmolt), the hemolymph ecdysteroid levels were measured. The hemolymph ecdysteroid levels increased in early premolt followed by greater peak compared with intermolt animals, whereas the levels in postmolt animals just after molting were very low (Fig. 5). As intermolt green and red morphs were resistant to ESA and MLA, the expression of EF2 was measured in YOs from naturally molting green morphs at the intermolt, premolt, and posmolt stages using quantitative PCR. Little changed during the examined EF2 molt cycles in animals during their natural molt. At intermolt, premolt, and posmolt molt stages, there is no a significant change in the expression of EF2 copy numbers in YOs tissue in green morphs (Data not showing).

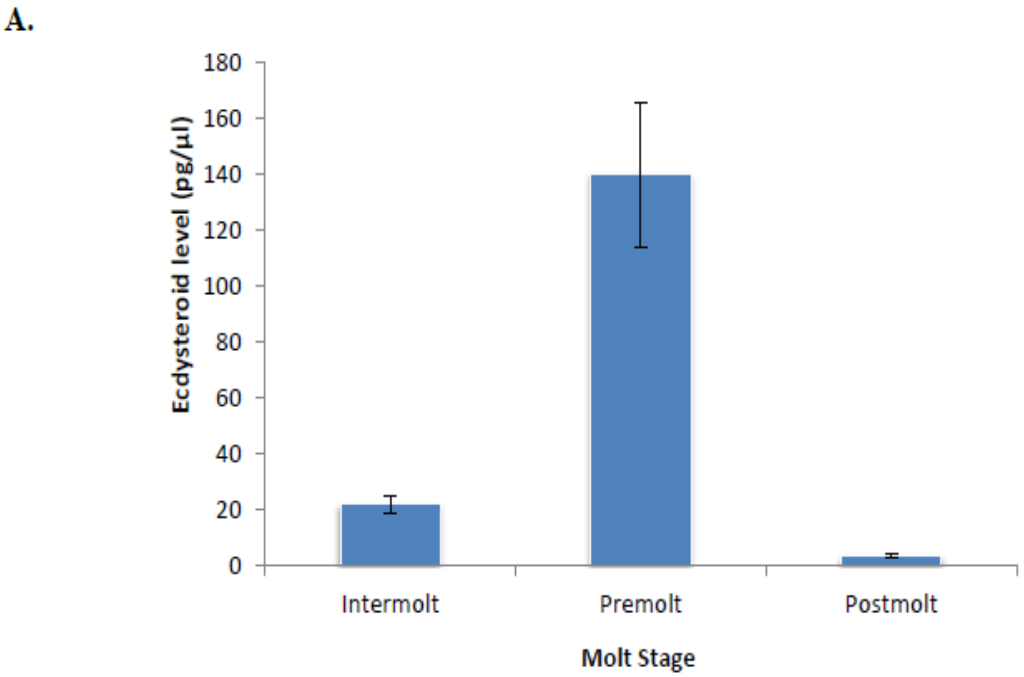

Figure (5): Effects of molting on hemolymph ecdysteroid levels *in C. maenas* YOs. Hemolymph was collected from spontaneously molting green morphs at 3 molt stages: intermolt, premolt, and posmolt. Data are presented as mean ± 1 S.E. (intermolt n = 62, premolt n= 18, and posmolt n = 4).

Effects of ESA on expression of Cm-MIH and Cm-EF2 in brain and thoracic ganglion from green and red morphs:

The main location for MIH synthesis in decapod crustaceans is the XO/SG complex in the eyestalks. The brain and thoracic ganglia were looked at as secondary sources of MIH because ESA did not cause molting in intermolt animals. Nested endpoint PCR results from intact intermolt animals showed that MIH was expressed in the brain and thoracic ganglia (Fig. 6). To measure the expression of MIH and EF2 in intact, 7-day, and 14-day ESA red and green morphs, the brain and thoracic ganglia of *C. maenas* were extracted. The expression of *Cm-MIH* and *Cm-EF2* in the brain and thoracic ganglia was unaffected by ESA. In the red and green morphs, *Cm-MIH* expression was maintained at intact levels. We come to the conclusion that the brain and thoracic ganglia function as secondary sources of MIH, which can make up for the loss of the eyestalks and prevent precocious molting (Fig. 7B, C). After the long-term experiments, YOs were harvested, and real-time PCR was used to measure the expression of EF2. The *Cm-EF2* examined in red and green morph showed little change in the ESA and MLA assays. In either the red or green morph of YOs tissue, EF2 copy numbers did not significantly change.

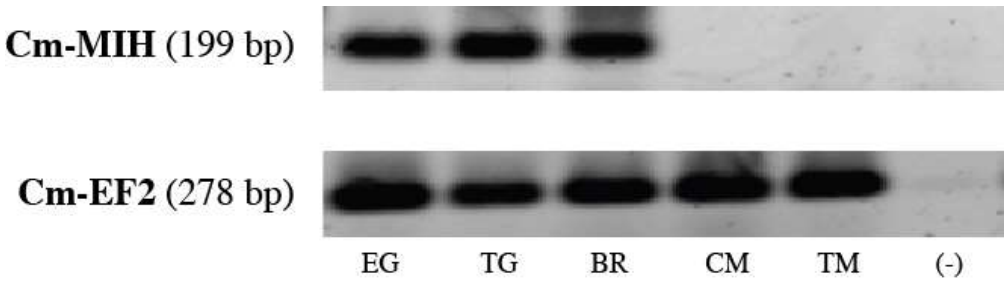

Figure (6): Expression of *Cm-MIH* and *Cm-EF2* in eyestalk ganglia, brain, muscle, and thoracic ganglion from intermolt *C. maenas*. Nested end-point PCR was used to detect *Cm- MIH* transcript in cDNA from brain, thoracic ganglion, and muscle (35 cycles for each round). A single round of PCR was used to detect *Cm-MIH* in eyestalk ganglia (35 cycles with the inner primer pair) and *Cm-EF2* in cDNA from brain, thoracic ganglion, and muscle.

The dependence of crustacean coloration on eyestalk variables has long been recognized (Pouchet, 1872; Shibley, 1968). Because chromatophores contain concentrated pigment, the majority of animals' bodies blanch when their eyestalks are removed (Shibley, 1968). According to Abramowitz (1937), Carlson (1936), Fingerman (1965), Kleinholz (1961), and Shibley (1968), the condition can be temporarily reversed by injecting eyestalk extracts into the animal. The fiddler crab Uca and the crayfish Astacus can both have their daily rhythmic color changes eliminated by eyestalk ablation (Brown, 1961). In 1951, Lenel and Veillet reported the changes in color after removing the eyestalk factors. This color shift was caused by the dissociation of the brown and green astaxanthin-protein complexes, not by an increase in the carotenoid astaxanthin accumulation. Our findings agreed with those of Lenel and Veillet. From the first two weeks until the end of the experiment, the ESA treatment group's green:red ratio showed a strong decline (Fig. 4). Intensity of red hue, which probably indicated the concentration of astaxanthin, was constant in ESA and MLA animals. As evidenced by low hemolymph ecdysteroid titers and the presence of the membranous layer at the conclusion of the experiment, green morphs stayed in intermolt and did not molt. The green: red ratio of MLA animals showed a trend toward decrease, but it did not differ significantly from intact animals (Fig. 4). This shows that MLA can affect the production and/or release of the neuroendocrine factor(s) in the eyestalk which regulate the transition from green to red. Further research is necessary to determine this factor's identity and mode of action eyestalks of *C. maenas*. According to Goodwin (1960) and Lenel and Veillet (1951), the epidermal chromatophores are impacted after the pigmentary layer of the new cuticle. According to Lenel and Veillet (1951), the dissociation of the brown and green astaxanthin-protein complexes was what caused the change in color rather than an increase in the carotenoid astaxanthin accumulation.

The main source of MIH in decapod crustaceans is the XO/SG complex. However, there are numerous reports of MIH expression in other tissues. Me-MIH-A is expressed in the eyestalk, whereas Me-MIH-B is expressed in the eyestalk, brain, thoracic ganglion, and ventral nerve cord (Tiu and Chan, 2007). According to Zhu et al. (2011), the eyestalk ganglia, brain, thoracic ganglion, and gonadal tissues of the swimming crab, *Portunus trituberculatus*, expressed MIH. In *Cancerpagurus*, MIH is expressed in the neurological

tissues including the optic nerve, ventral nerve cord, and thoracic/abdominal ganglion. The findings of the nested PCR analysis (Fig. 6) clearly demonstrate the presence of PCR products with the predicted size of MIH (199 bp) in the brain and thoracic ganglia. however, we did take into account the potential for MIH mRNA or cDNA to contaminate PCR reactions of thoracic ganglia and brain preps. Although we can't completely rule it out, this is less likely given that neither the muscle cDNAs nor the water control produced PCR products (Fig. 6).

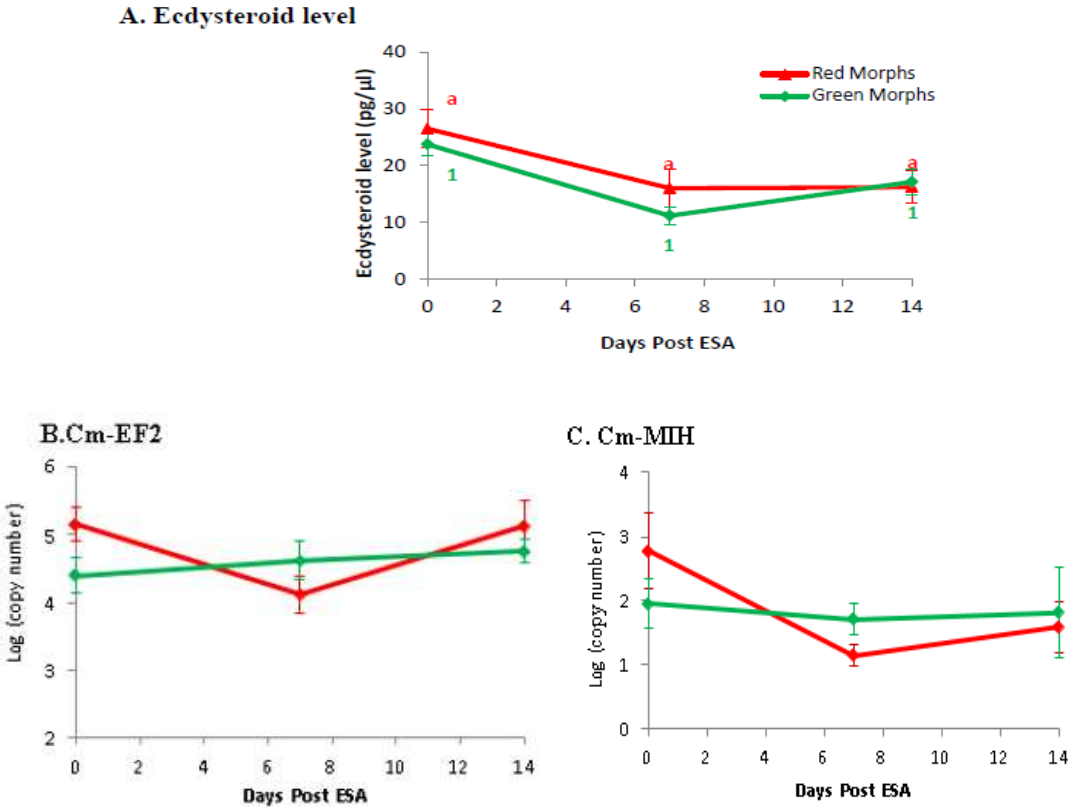

Figure (7): Effects of ESA on hemolymph ecdysteroid (A), and expression of *Cm-EF2* (B), and *Cm-MIH* (C), in brain and thoracic ganglion from red and green morphs. Hemolymph and tissues were collected from intact (Day 0) and 7-day and 14-day ESA red and green morphs (see Materials and methods). Letters and numbers indicate significant differences between the control (intact) and ESA in hemolymph level (A), red morph at $p < 0.05$ (a & b) and green m o r p h at $p < 0.001$ (1, 2 & 3). The samples from the brain and thoracic ganglion were combined for qPCR.

Conclusions:

Eyestalk neuroendocrine factor(s) control the transition from the green to the red morph type, as the pigmentation change was accelerated by ESA. The shift takes place in intermolt animals, therefore MIH does not appear to be involved. It's intriguing that the color shift wasn't brought on by an increase in the red pigment. Instead, the green color is reduced, revealing the red pigment and making it more apparent. Experiments by ESA and MLA had no effect. *C. maenas* is resistant to ESA. MIH transcript was detected by nested endpoint RT-PCR in the brain and thoracic ganglia of intermolt animals. The

MIH gene was not transcriptionally controlled by the loss of the eyestalks, as evidenced by the fact that MIH expression was similar between the color morphs and that ESA had minimal impact on MIH transcript levels. The evidence suggests that when the main supply of MIH is eliminated by ESA, MIH released by brain and thoracic ganglion neurons is enough to prevent molt induction.

REFERENCES

Abramowitz, A. A. (1937). The chromatophorotropic hormone of the Crustacea: standardization, properties, and physiology of the eyestalk glands. Biol. Bull. 72: 344-365.

Brown, F.A., Jr. (1961). Physiological rhythms. In: Waterman, T.H. (Ed.) The Physiology of Crustacea, vol. 2. Academic Press, New York, pp. 401-430

Carlson, S.P. (1936). Color changes in brachyuran crustaceans, especially in Uca pugilator. Proc. Roy. Physiograph. Soc. Lund. 6: 63-80.

Chang, E.S. (1989). Endocrine regulation of molting in Crustacea. Rev. Aquatic Sci. 1, 131-158.

Chang, E.S. and Mykles, D.L. (2011). Regulation of crustacean molting: A review and our perspectives. Gen. Comp. Endocrinol. 172: 323-330.

Covi, J. A.; Bader,B., D.; Chang, E., S. and Mykles, D., L. (2010). Molt cycle regulation of protein synthesis in skeletal muscle of the blackback land crab, *Gecarcinus lateralis*, and the differential expression of myostatin-like factor during atrophy induced by mplting or unweighting. J.Exp. Biol. 213:172-183.

Covi, J. A.; Chang, E.S. and Mykles, D.L. (2009). Conserved role of cyclic nucleotides in the regulation of ecdysteroidogenesis by the crustacean molting gland. Comp. Biochem. Physiol. 152A: 470-477.

Covi, J. A.; Chang, E.S. and Mykles, D.L. (2012). Neuropeptide signaling mechanisms in crustacean and insect molting glands. Invert. Reprod. Dev. 56: 33-49.

Fingerman, M. (1965). Chromatophores. Physiol. Rev. 45.

Goodwin, T.W. (1960). Biochemistry of pigments. In: Waterman, T.H. (Ed.) The Physiology of Crustacea, vol. 1. Academic Press, New York. pp: 101-140

Grosholz, E.D. and Ruiz, G.M. (1996). Predicting the impact of introduced marine species: Lessons from the multiple invasions of the European green crab, *Carcinus maenas*. Biol. Conserv. 78: 59-66.

Grosholz, E.D.; Ruiz, G.M. (1995). Spread and potential impact of the recently introduced European green crab, *Carcinus maenas*, in Central California. Mar. Biol. 122: 239-247.

Hanfling, B.; Edwards, F. and Gherardi, F. (2011). Invasive alien Crustacea: dispersal, establishment, impact and control. Biocont. 56: 73-595.

Hopkins, P.M. (2012). The eyes have it: A brief history of crustacean neuroendocrinology. Gen. Comp. Endocrinol. 175: 357-366.

Kingan, T.G. (1989). A competitive enzyme-linked immunosorbent assay - Applications in the assay of peptides, steroids, and cyclic nucleotides. Anal. Biochem. 183: 283-289.

Klein, J.M.; Mangerich, S.; De Kleijn, D.P.V.; Keller, R. and Weidemann, W.M. (1993). Molecular cloning of crustacean putative molt-inhibiting hormone (MIH) precursor. FEBS Lett. 334: 139-142.

Kleinholz, L.H. (1961). Pigmentary effectors. In: Waterman, T.H. (Ed.) Physiol. Crust. 2.Academic Press, New York. pp: 133-169

Lachaise, A.; Le Roux, A.; Hubert, M. and Lafont, R. (1993). The molting gland of crustaceans: localization, activity, and endocrine control. J. Crust. Biol. 13: 198-234.

Lee, S. G. and Mykles, D.L. (2006). Proteomics and signal transduction in the crustacean molting gland. Integr. Comp. Biol. 46: 965-977.

Lee, S.G.; Bader, B.D.; Chang, E.S. and Mykles, D.L. (2004). High-throughput proteomic approaches for identifying molt-associated proteins in crustacean molting gland. Integr. Comp. Biol. 44: 717.

Lee, S.G.; Bader, B.D.; Chang, E.S. and Mykles, D.L. (2007a). Effects of elevated ecdysteroid on tissue expression of three guanylyl cyclases in the tropical land crab *Gecarcinus lateralis*: possible roles of neuropeptide signaling in the molting gland. J. Exp. Biol. 210: 3245-3254.

Lee, S.G.; Kim, H.W. and Mykles, D.L. (2007b). Guanylyl cyclases in the tropical land crab, *Gecarcinus lateralis*: Cloning of soluble (NO-sensitive and -insensitive) and membrane receptor forms. Comp. Biochem. Physiol. 2D: 332-344.

Lenel, R., Veillet, A. (1951). Effects de l'ablation des pédoncules oculaires sur les pigments caroténoïdes du crabe Carcinus maenas. C. R. Acad. Sci. Paris 233, 1064-1065.

Lu, W.Q.; Wainwright, G.; Olohan, L.A.; Webster, S.G.; Rees, H.H. and Turner, P.C. (2001). Characterization of cDNA encoding molt-inhibiting hormone of the crab, *Cancer pagurus*; expression of MIH in non-X-organ tissues. Gene 278: 149-159.

McGaw, I.J. and Naylor, E. (1992a). Distribution and rhythmic locomotor patterns of estuarine and open-shore populations of *Carcinus maenas*. J. Mar. Biol. Assoc. U. K. 72, 599-609.

McGaw, I.J. and Naylor, E. (1992b). Salinity preference of the shore crab *Carcinus maenas* in relation to coloration during intermolt and to prior acclimation. J. Exp. Mar. Biol. Ecol. 155: 145-159.

Medler, S.; Brown, K.J.; Chang, E.S. and Mykles, D.L. (2005). Eyestalk ablation has little effect on actin and myosin heavy chain gene expression in adult lobster skeletal muscles. Biol. Bull. 208: 127-137.

Mykles, D. L.; Adams, M.E.; Gade, G.; Lange, A.B.; Marco, H.G. and Orchard, I. (2010). Neuropeptide action in insects and crustaceans. Physiol. Biochem. Zool. 83:

836-846.

Mykles, D.L. (1997). Crustacean muscle plasticity: Molecular mechanisms determining mass and contractile properties. Comp. Biochem. Physiol. 117B, 367-378.

Mykles, D.L. (2001). Interactions between limb regeneration and molting in decapod crustaceans. Am. Zool. 41: 399-406.

Mykles, D.L. (2011). Ecdysteroid metabolism in crustaceans. J. Steroid Biochem. Molec. Biol. 127: 196-203.

Nakatsuji, T.; Lee, C.Y. and Watson, R.D. (2009). Crustacean molt-inhibiting hormone: Structure, function, and cellular mode of action. Comp. Biochem. Physiol. 152A: 139-148. Neuropeptide action in insects and crustaceans. Physiol. Biochem. Zool. 83: 836-846.

Mykles, D.L. (2011). Ecdysteroid metabolism in crustaceans. J. Steroid Biochem. Molec. Biol. 127: 196-203.

Pouchet, G. (1872). Sur les rapides changements de coloration provoqués expérimentalement, chez les Crustacés et sur les colorations bleues des poissons. J. Anat. 8: 401-407.

Reid, D.G.; Abello, P.; Kaiser, M.J. and Warman, C.G. (1997). Carapace colour, inter-moult duration and the behavioural and physiological ecology of the shore crab Carcinus maenas. Estuar. Coast. Shelf Sci. 44: 203-211.

Shibley, G.A. (1968). Eyestalk function in chromatophore control in a crab, Cancer magister. Physiol. Zool. 41: 268-279.

Skinner, D. M. (1985). Molting and regeneration, in The Biology of Crustacea, Bliss, D.E. and Mantel, L.H., Editors. Academic Press: New York. pp: 43-146.

Skinner, D.M., Graham, D.E. (1972). Loss of limbs as a stimulus to ecdysis in Brachyura (true crabs). Biol. Bull. 143: 222-233.

Tamone, S.L.; Taggart, S.J.; Andrews, A.G.; Mondragon, J. and Nielsen, J.K. (2007). The relationship between circulating ecdysteroids and chela allometry in male tanner crabs: Evidence for a terminal molt in the genus Chionoecetes. J. Crustacean Biol. 27, 635-642.

Tiu, S.H.K. and Chan, S.M. (2007). The use of recombinant protein and RNA interference approaches to study the reproductive functions of a gonad-stimulating hormone from the shrimp *Metapenaeus ensis*. J. FEBS. 274: 4385-4395.

Webster, S.G.; Keller, R. and Dircksen, H., (2012). The CHH-superfamily of multifunctional peptide hormones controlling crustacean metabolism, osmoregulation, moulting, and reproduction. Gen. Comp. Endocrinol. 175: 217-233.

Zhu, D.F.; Hu, Z.H. and Shen, J.M. (2011). Moult-inhibiting hormone from the swimming crab, *Portunus trituberulatus* (Miers, 1876); PCR cloning, tissue distribution, and expression of recombinant protein in Escherichia coli (Migula, 1895). Crus. 84: 1481-1496.

التعبير الجيني عن الهرمون المثبط للانسلاخ الـMIH في الدماغ والعصبونات الصدرية لسرطان الـ *Carcinus maenas*

علي مفتاح أبو حجر

قسم الأنسجة وعلم الوراثة، كلية الطب البشري، الجامعة الأسمرية الإسلامية، ليبيا.

الخلاصة:

تنتج غدد تحت العينين في القشريات هرمون الببتيد العصبي المعروف باسم الهرمون المثبط للانسلاخ (MIH) والذي يتحكم في عملية الانسلاخ عن طريق منع غدة الانسلاخ من إنتاج هرمون الاكديستيرون (هرمون الانسلاخ). عادة عملية إزالة غدد تحت العينين (ESA) تحفز عملية الانسلاخ، ومع ذلك فإن السرطانات الخضراء البالغة مقاومة لـعملية الإزالة (ESA). تؤدي عملية إزالة الغدد تحت العينين إلى ارتفاع طفيف في معدلات هرمون الاكديستيرون، وعلى الرغم من أن الحيوانات لا تدخل على الفور في مرحلة ما قبل الانسلاخ إلا أن بعض الحيوانات منزوعة الغدد تحت العينين تدخل بعد عدة أشهر في عملية الانسلاخ، في حين أن الغالبية العظمي لا تدخل على الإطلاق في عملية الانسلاخ. مما يؤكد أن الهرمون المثبط للانسلاخ (MIH) أفرز من أجزاء أخرى من الجهاز العصبي، ولا سيما الدماغ أو العصبونات العصبية الصدرية. وجدت نسخة من هذا الهرمون MIH في الدماغ والعصبونات الصدرية لعينات الـ PCR وتم التحقق منها منتجات PCR على أنها MIH عن طريق التفاعل التسلسلي. وتمت دراسة تأثير الـESA على تعبير الـMIH باستخدام الـPCR الكمي. وكان تعبير الـMIH متشابهًا بين الأشكال اللونية والـESA كان له تأثير ضئيل على مستويات الـ MIH، مما يشير إلى أن فقدان هذه الغدد لم يؤثر على تنظيم جين هرمون الـMIH وتشير البيانات إلى أنه عندما يتم التخلص من الإمداد الرئيسي لـ MIH بواسطة الـESA، فإن الـMIH الذي يتم إطلاقه بواسطة الخلايا العصبية في الدماغ أو العصبونات الصدرية يكون كافياً لمنع تحفيز عملية الانسلاخ.

الكلمات المفتاحية: هرمون الـMIH- هرمون الاكديستيرون- العصبونات الصدرية- الدماغ- إزالة الغدد تحت العينين الـESA-